

Supporting Information for:

Bifunctional Ligand Design for Modulating Mutant p53 Aggregation in Cancer

Jessica J. Miller,^a Anaïs Blanchet,^b Christophe Orvain,^b Lucienne Nouchikian,^c Yasmin Reviriot,^a Ryan M. Clarke,^a Diego Martelino,^a Derek Wilson,^c Christian Gaiddon,^{*b} Tim Storr^{*a}

^aSimon Fraser University, Department of Chemistry, 8888 University Drive, Burnaby BC V5A 1S6, Canada

^bInserm U1113, Université de Strasbourg, Molecular Mechanisms of Stress Response and Pathologies, Strasbourg, France

^cYork University, Chemistry Department, 6 Thompson Road, Toronto, Ontario, M3J 1L3, Canada

Email: gaiddon@unistra.fr, tim_storr@sfu.ca

1. Experimental.....	S2-11
2. Synthetic scheme for L^I	S11
3. Synthetic scheme for L^H	S11
4. ¹ H NMR for L^I in CD ₂ Cl ₂	S12
5. ¹ H NMR for L^H in CD ₂ Cl ₂	S13
6. ¹³ C NMR for L^I in CDCl ₃	S14
7. ¹³ C NMR for L^H in CD ₂ Cl ₂	S15
8. Light scattering of wild-type p53 upon treatment with L^I and L^H	S16
9. Molecular weight distribution of mutant p53 by gel electrophoresis.....	S16
10. Immunofluorescence staining with Thioflavin T.....	S17
11. pK _a determination for L^I	S17
12. pK _a determination for L^H	S18
13. Speciation diagram of L^I	S18
14. Speciation diagram of L^H	S19
15. Zn K _d determination for L^I	S19
16. Zn K _d determination for L^H	S20
17. Speciation diagram of Zn L^I	S20
18. Speciation diagram of Zn L^H	S21
19. Calculated pK _a values for L^I and L^H using HypSpec.....	S21
20. Calculated pM and logK values for L^I and L^H using HypSpec.....	S21
21. Crystallographic information for Zn L^I Cl and Zn L^H Cl.....	S22
22. Ligand control for imaging of intracellular Zn ²⁺ levels.....	S22

23. Immunoprecipitation of mutant p53 with conformation-specific antibodies.....	S23
24. Upregulation of p53 transcription factors by rtPCR.....	S23
25. Heat map of NCI-60 GI ₅₀ results.....	S24
26. Mean GI ₅₀ and LC ₅₀ values from the NCI-60 screen.....	S25
27. <i>In vitro</i> cytotoxicity of L ^I and L ^H in the stomach cancer cell lines.....	S25
28. Cleaved caspase 3 Western blot on the AGS cell line.....	S25
29. Quantification of relative cleaved caspase 3 levels upon L ^I and L ^H treatment.....	S26
30. Quantification of relative cleaved caspase 3 levels upon cotreatment with L ^I and oxaliplatin.....	S26
31. Quantification of AIF nuclear localization upon L ^I and L ^H treatment.....	S27
32. Expression levels of PUMA and BAX upon co-treatment with L ^I and oxaliplatin.....	S27
33. Classification system for organoid model (image example).....	S28
34. Classification system for organoid model (table).....	S28
35. Organoid immunofluorescence with cleaved caspase 3.....	S29
36. Organoid immunofluorescence and viability over a 23-day period.....	S30
37. Tolerability of L ^I in normal mice.....	S31

Experimental

Materials and Methods. All chemicals used were purchased from Sigma Aldrich at the highest grade available and were further purified whenever necessary.¹ All compounds were dried under vacuum for 1 week before *in vitro* cytotoxicity testing. ¹H and ¹³C NMR were recorded on Bruker-AV-400, 500, and 600 instruments. Elemental analyses (C, H, N) were performed by Mr. Paul Mulyk at Simon Fraser University on a Carlo Erba EA 1110 CHN elemental analyzer. Mass spectra (negative ion) were obtained on an Agilent 6210 time-of-flight electrospray ionization mass spectrometer. Electronic absorption spectra were obtained on a Cary 5000 spectrophotometer. Scatter experiments were carried out on a Synergy 4 MultiDetection microplate reader (BioTek). TEM images were obtained on a STEM 1 – FEI Tecnai Osiris transmission electron microscope. Immunofluorescence experiments were imaged using a fluorescence microscope (Axio Imager M2 Zeiss) coupled to a Hamamatsu’s camera Orca Flash 4v3, using the ApoTome.2 (Zeiss) function.

4-(benzo[d]thiazol-2-yl)-2-iodophenol To a solution of 4-hydroxy-3-iodobenzaldehyde (0.59 g, 2.39 mmol) in EtOH (13 mL) 2-aminothiophenol (0.30 g, 2.39 mmol) was added. Aqueous hydrogen peroxide (1.5 mL, 30%, 6 molar equivalents) and 37% aqueous HCl (1.9 eq) were added. Upon stirring for 2 hours, a green

precipitate formed. The precipitate was filtered, washed with cold ethanol, and dried in vacuo. Yield: 0.80 g, 95%. ^1H NMR (400 MHz, MeOD): δ = 8.47 (d, J = 2.2 Hz, 1H), 8.01 - 7.97 (m, 2H), 7.94 (dd, J = 8.5 Hz and 2.2 Hz, 1H), 7.54 (td, J = 8.4 and 1.2 Hz, 1H), 7.44 (td, J = 8.3 and 1.2 Hz, 1H), 6.98 (d, J = 8.5 Hz, 1H). ^{13}C { ^1H } NMR (400 MHz, MeOD) δ = 166.9, 159.8, 153.6, 138.0, 134.4, 128.7, 126.2, 125.0, 122.0, 121.4, 114.50, 83.8. Anal. Calcd (%) for $\text{C}_{13}\text{H}_8\text{INOS}$: C, 44.21; H, 2.28; N, 3.97; found: C, 44.43; H, 2.23; N, 4.01. Calcd for M, 352.9371; found, 352.9372.

4-(benzo[d]thiazol-2-yl)-2-((bis(pyridin-2-ylmethyl)amino)methyl)-6-iodophenol (L^I). Paraformaldehyde (0.107 g, 3.57 mmol) was added to a solution of di-(2-picolyl)amine (0.339 g, 1.70 mmol) in THF (14 mL) and refluxed for 1 hour. 2-(4-hydroxy-3-iodo)benzothiazole (0.60 g, 1.70 mmol) in 12 mL of THF was added, and the solution was refluxed for an additional 72 hrs. The THF was removed in vacuo and the resulting solid was recrystallized in hot methanol to afford a white precipitate. The precipitate was removed using vacuum filtration and washed with cold methanol. Yield: 0.29 g, 31%. ^1H NMR (500 MHz, CD_2Cl_2): δ = 8.63 (dd, J = 4.9, 1.8 Hz, 2H), 8.44 (d, J = 2.2 Hz, 1H), 8.03 - 7.99 (m, 1H), 7.96 - 7.93 (m, 1H), 7.88 (d, J = 2.2 Hz, 1H), 7.72 (td, J = 7.7, 1.8 Hz, 2H), 7.51 (dd, J = 8.3, 7.2 Hz, 1H), 7.40 (dd, J = 8.2, 7.3 Hz, 1H), 7.36 (d, J = 7.8 Hz, 2H), 7.25 (dd, J = 7.5, 4.9 Hz, 2H), 3.97 (s, 4H), 3.94 (s, 2H). ^{13}C { ^1H } NMR (400 MHz, CD_2Cl_2): δ = 166.2, 159.9, 157.9, 154.2, 148.8, 137.6, 136.8, 134.9, 129.8, 126.2, 126.1, 124.8, 123.9, 123.1, 122.6, 122.3, 121.5, 85.8, 58.8, 56.8. Anal. Calcd (%) for $\text{C}_{26}\text{H}_{21}\text{IN}_4\text{OS}$: C, 55.33; H, 3.75; N, 9.93; found: C, 55.40; H, 3.71; N, 9.98. HR-MS: Calcd for $[\text{M} + \text{H}]^+$, 565.0559; found, 565.0520.

4-(benzo[d]thiazol-2-yl)-2-((bis(pyridin-2-ylmethyl)amino)methyl)phenol (L^H). Paraformaldehyde (0.31 g, 10.9 mmol) was added to a solution of di-(2-picolyl)amine (1.04 g, 5.45 mmol) in EtOH (40 mL) and refluxed for 1 hour. 2-(4-hydroxy)benzothiazole (1.19 g, 5.45 mmol) in 35 mL of EtOH was added, and the resulting solution was heated at a reflux for an additional 48 hrs. The solvent was removed to give a dark gray residue that was purified by silica gel column chromatography using EtOAc/iPrOH/ NH_4OH (75:20:5) as eluent to yield a brown solid. Yield: 0.84 g, 35%. ^1H NMR (400 MHz, CD_2Cl_2): δ = 8.56 (dd, J = 4.9, 1.8 Hz, 2H), 7.96 (dd, J = 8.2, 1.2 Hz, 1H), 7.91 - 7.87 (m, 3H), 7.65 (td, J = 7.7, 1.8 Hz, 2H), 7.45 (dd, J

= 8.3, 7.2 Hz, 1H), 7.36 – 7.31 (m, 3H), 7.19 (dd, $J = 7.5, 4.9$ Hz, 2H), 6.99 – 6.96 (m, 1H), 3.92 (s, 4H), 3.89 (s, 2H). $^{13}\text{C}\{^1\text{H}\}$ NMR (500 MHz, CD_2Cl_2): $\delta = 168.5, 161.4, 158.6, 154.7, 149.1, 137.2, 135.2, 130.1, 129.1, 126.5, 124.9, 124.8, 124.4, 123.5, 122.8, 122.6, 121.9, 117.5, 59.2, 57.0$. Anal. Calcd (%) for $\text{C}_{26}\text{H}_{22}\text{N}_4\text{OS}\cdot\text{H}_2\text{O}$: C, 68.40; H, 5.30; N, 12.27; found: C, 68.73; H, 5.17; N, 12.47. HR-MS: Calcd for $[\text{M} + \text{H}]^+$, 439.1593; found, 439.1567.

$[(\text{L}^{\text{I}})\text{Zn}^{\text{II}}]\text{Cl}$ Into a solution of L^{I} (0.02 g, 0.04 mmol) in MeOH (5 mL), KOH (2 mg, 0.04 mmol) and ZnCl_2 (5 mg, 0.04 mmol) were added and the solution was stirred for 1 hour. The solution was filtered through Celite to remove precipitated KCl and the complex was precipitated from cold diethyl ether. The resulting white solid was collected using vacuum filtration and washed with cold MeOH. Yield: 0.019 g, 73%. ^1H NMR (400 MHz, $(\text{CD}_3)_2\text{SO}$): $\delta = 9.01$ (d, $J = 5.1$ Hz, 2H), 8.09 (d, $J = 2.4$ Hz, 1H), 8.06 – 7.99 (m, 3H), 7.90 – 7.87 (m, 1H), 7.74 (d, $J = 2.4$ Hz, 1H), 7.63 – 7.58 (m, 2H), 7.51 (d, $J = 7.8$ Hz, 2H), 7.46 (dd, $J = 8.3, 7.2$, 1H), 7.34 (dd, $J = 8.2, 7.2$ Hz, 1H), 4.12 (d, $J = 3.2$ Hz, 4H), 3.76 (s, 2H). Crystals suitable for X-ray diffraction experiments were obtained by slow diffusion of a concentrated CH_2Cl_2 solution into hexanes.

$[(\text{L}^{\text{H}})\text{Zn}^{\text{II}}]\text{Cl}$ Into a solution of L^{H} (0.05 g, 0.11 mmol) in MeOH (5 mL), KOH (6.4 mg, 0.11 mmol) and ZnCl_2 (15.5 mg, 0.11 mmol) were added and the solution stirred for 1 hour. The solution was filtered through Celite to remove precipitated KCl and the complex was precipitated from cold diethyl ether. The resulting white solid was collected using vacuum filtration and washed with cold MeOH. Yield: 0.042 g, 71%. ^1H NMR (400 MHz, $(\text{CD}_3)_2\text{SO}$): $\delta = 9.07$ (d, $J = 5.4$ Hz, 1H), 7.99 (d, $J = 7.9$ Hz, 1H), 7.86 (d, $J = 8.1$ Hz, 1H), 7.76 (d, $J = 2.5$ Hz, 1H), 7.65 (t, $J = 6.4$ Hz, 2H), 7.60 (t, $J = 7.1$ Hz, 2H), 7.44 (t, $J = 7.6$ Hz, 1H), 7.31 (t, $J = 7.6$ Hz, 1H), 6.49 (d, $J = 8.6$ Hz, 1H), 4.08 (s, 4H), 3.76 (s, 2H). Crystals suitable for X-ray diffraction experiments were obtained by slow diffusion of a concentrated CH_2Cl_2 solution into hexanes.

X-Ray crystallography. X-ray structure determinations were performed on a Bruker APEX II Duo diffractometer with graphite monochromated Mo $\text{K}\alpha$ radiation. A transparent block crystal was mounted on a 150 μm MiteGen sample holder. Data were collected at 293 K to a maximum 2θ value of $\sim 60^\circ$. Data were collected in a series of ϕ and ω in 0.50° widths with 10.0 s exposures. The crystal-to-detector distance

was 50 mm. The structure was solved by intrinsic phasing² and refined using ShelXle.³ All non-hydrogen atoms were refined anisotropically. All C-H hydrogen atoms were placed in calculated positions but were not refined. ZnL^ICl crystalizes with only one molecule of ZnL^ICl in the asymmetric unit, while ZnL^HCl crystalizes with two molecules in the asymmetric unit.

Acidity and Stability Constant Determination. Aqueous acidity constants (pK_a) for L^I and L^H were measured using variable pH titrations monitored by UV-visible spectroscopy between 200 and 600 nm as a function of pH. Solutions of both ligands (12.5 μ M) were prepared in 0.1 M NaCl pH 3. Due to the limited aqueous solubility, solutions of 20% MeOH in H₂O were prepared. Small aliquots of 0.1 M NaOH were titrated into the solution to adjust the pH and at least 30 UV-vis spectra were collected in the pH 3-11 range. Spectral data were analyzed using HypSpec (Protonic Software, UK).⁴ Similarly, metal stability constants were obtained by titrating a solution containing 12.5 μ M ligand, 12.5 μ M Zn(ClO₄)₂·6H₂O, 0.1 M NaCl and 0.1 M NaOH to adjust the pH. At least 30 UV-vis spectra were collected in the pH 3-11 range. Known metal hydrolysis constants were included in the HypSpec simulations as constant values.⁵ Stability constants were calculated using the HypSpec computer program and metal speciation plots were created using the HySS2009 program (Protonic Software, UK).⁴

Increasing intracellular levels of Zn²⁺ in the p53 Y220C cell line NUGC3. NUGC3 cells (40,000 cells/well) were plated on glass slides treated with poly-L-lysine in 12-well plates. After 48 hours, cells were washed 2x 5 minutes in serum-free media and incubated with 1 μ M FZ3-AM⁶ for 20 minutes at 37°C. Cells were then washed 2x 5 minutes in Earle's balanced salt solution (EBSS)/H (-) Ca/Mg containing the indicated treatments (ZnCl₂ = 50 μ M, L^I = L^H = pyrithione = 50 μ M) and incubated for 2 hours at 37 °C before imaging. Cells were imaged using a Nikon ApoTome microscope (Nikon, France). FZ3-AM and Hoechst 33342 were excited at 488 nm (argon laser) and 790 nm (Chameleon Ti:sapphire laser), respectively. Imaging was performed in under ten minutes to avoid alteration of cell physiology upon imaging at room temperature. To determine the change in fluorescence, each image was processed using ImageJ Software (National Institutes of Health, Bethesda, MD) and integrated to represent the cumulative fluorescence for a single cell - processing included adjustment of exposure and contrast to eliminate

autofluorescence of the support. To avoid autofluorescence of the cells, each image was background-subtracted using the non-treated control. All images taken within an experiment were processed identically. Cells were analyzed upon treatment with 50 μ M pyrithione (PYR)/ZnCl₂ (1:1) as a positive control (Figure 3). Statistical differences were analyzed using 1-way ANOVA with multiple comparisons. Bartlett's test shows unequal variance. The number of cells analyzed in each trial is 100. Three replicate experiments were performed independently of one another.

Site-Directed Mutagenesis. The plasmid encoding the human p53 (residues 94-312) gene was a gift from Cheryl Arrowsmith.⁷ Four mutations to the p53 gene (M133L/V203A/N239Y/N268D) were introduced to increase stability.⁸ All p53 mutants were prepared by PCR according to standard protocols⁹ using primers purchased from Eurofins Operon. Site directed mutant plasmids were obtained using the Quikchange protocol (Agilent Technology). DNA polymerase (Q5) and DpnI were obtained from New England Biolabs. PCR reaction mixtures were transformed into chemically competent DH5 α *E. coli* and plated on ampicillin-supplemented agar plates. Single colonies obtained from overnight incubation at 37 °C were grown in Luria-Bertani (LB) broth for 16 hours (37 °C). Plasmid DNA was purified using a Qiagen plasmid spin MiniPrep kit and sequenced by Eurofins Operon Sequence read service.

Protein Expression and Purification. Proteins were expressed using *E. coli* strain BL21-pLysS cells (ThermoFisher). Expression cultures containing 100 μ g/mL ampicillin were inoculated from an overnight culture and grown at 37 °C to an OD₆₀₀ of 0.7. Overnight induction at 15 °C with 0.3 mM IPTG followed. Cells were harvested by centrifugation at 6500 rpm for 20 mins. Cell pellets were resuspended in 50 mM Tris, pH 6.5, 300 mM NaCl, 10% glycerol, 1% Triton X-100, 5 mM imidazole, 6 mM MgSO₄, 1 mM PMSF, and 5 mM β -mercaptoethanol and lysed using ultrasonication. Cellular debris was isolated by centrifugation at 14000 rpm for 30 minutes and incubated with Talon® beads (cobalt-nitrilotriacetic acid) at 4 °C for 30 minutes. The Talon beads were transferred to a column, washed with 2 \times 20 mL washing buffer (50 mM tris, pH 6.5, 500 mM NaCl, 10% glycerol, 10 mM imidazole, 0.5 mM TCEP, 1 mM PMSF, and 5 mM β -mercaptoethanol), and eluted with elution buffer (washing buffer containing 500 mM imidazole).⁹ Protein

concentration was determined spectrophotometrically using the reported extinction coefficient $\epsilon_{280} = 17,130 \text{ cm}^{-1}$.¹⁰

Light Scattering. To monitor the effect of L^I and L^H on the aggregation of p53 Y220C, we measured light scattering by monitoring the changes in absorbance at 500 nm using a Synergy 4 MultiDetection microplate reader (BioTek). Experiments were carried out at 37 °C, with 30 seconds of agitation before each read. Spectra were taken in five-minute intervals. Protein concentration was 5 μM in 30 mM Tris, 150 mM NaCl at pH 7.4. 5% DMSO was used in the buffer to pre-dissolve L^I and L^H at final concentrations of 5 and 10 μM . Each experiment contained 8 replicates per condition, and values are represented as mean \pm SD.

Transmission Electron Microscopy. p53 Y220C (μM) was incubated at 37 °C with agitation at 100 rpm for indicated time points in the absence (NT) or presence of 5 μM L^I or L^H . The protein and ligands were dissolved in a buffer containing 30 mM Tris, 150 mM NaCl, pH 7.4 with 5% DMSO. Samples of 10 μL were adsorbed onto freshly glow-discharged formvar coated copper grids, rinsed with deionized water to remove NaCl crystals, and stained with 1% uranyl acetate. Images were taken on a STEM 1 – FEI Tecnai Osiris transmission electron microscope.

Immunofluorescence (A11, ThT, and AIF). Cells were plated at a density of 600,000 cells per well in 6-well plates and treated with L^I , L^H , or an equivalent volume of DMSO for 24 hours. The cell culture medium was removed and 2 mL of fixation buffer (3.7% paraformaldehyde in PBS) was added to each well and incubated for 10 minutes at room temperature. Fixation buffer was removed, and wells were washed twice with PBS followed by incubation with 2 mL of permeabilization buffer (0.2% Triton X-100 in PBS) for 5 minutes. Wells were washed 2x10 min with PBS and blocking solution (10% normal goat serum in PBS) was added for 2 hours. The cells were simultaneously labelled with mouse monoclonal anti-human p53 DO-1 primary antibody (1:1000) and an oligomer-specific primary antibody, A11 (1:1000) for the aggregation studies overnight in the dark at 4 °C. For apoptosis detection, cells were labelled with the primary antibody AIF (1:100, Invitrogen). Cells were washed 3x with PBS followed by labelling with Alexa 568- conjugated goat anti-mouse (Invitrogen) and Alexa 647- conjugated goat anti-rabbit (Invitrogen) secondary antibodies (1:2,000) for 1.5 hours at room temperature in the dark. In the case of Thioflavin T

labelling, a 1 mM solution of ThT was added to the wells following labelling with secondary antibodies, washed with 2 mL of 70% ethanol to remove excess ThT, followed by washing with water. The cells were washed three times with PBS, followed by subsequent nuclei staining using DAPI (Sigma). The cover slips were mounted using Fluorsave (Fisher Scientific) and allowed to dry overnight, followed by analysis using a fluorescence microscope Olympus AX60-PS coupled to ProgRes® MF^{cool} JENOPTIK camera.

Native Mass Spectrometry. Recombinant p53-Y220C samples were thawed and dialysed in 200 mM ammonium acetate, and protein concentrations were measured using a Thermo Scientific NanoDrop Spectrophotometer. L^I and L^H were stored as DMSO stocks at 50 mM. Native MS experiments were performed on 3 μM p53-Y220C with L^I or L^H ratios of 2, 5, 10 and 25 equivalents. Each sample was incubated at room temperature for 2 hours. The final DMSO concentration in each sample is 0.2%. All MS data were acquired on a quadrupole ion mobility time-of-flight (TOF) mass spectrometer (Synapt G2S HDMS, Waters, Milford, MA, USA). Ions were produced by positive electrospray ionization (ESI) with a capillary voltage of 2 kV. The source temperature was set to 120 °C, with a sampling cone set to 150 V and the extraction cone set to 50 V. The trap cell containing argon gas was set at a pressure of 3.14×10^{-2} mbar. Trap and transfer collision energies were set to 20 V and 10 V respectively. The TOF pressure operated at 1.25×10^{-6} mbar.

Western Blot Analysis. For molecular weight distribution analysis, a solution of mutant p53-y220c was prepared at a concentration of 8 μM in 30 mM Tris, 150 mM NaCl at pH 7.4. Solutions in the presence of two equivalents of L^I and L^H were prepared and all samples were incubated for 2 hours at 37 °C with constant agitation at 180 rpm. Electrophoresis to separate protein aggregates was employed using 10-20% Mini-PROTEAN® Tris-Tricine Precast Gels (Bio-Rad) at 100 V for 100 min. Using a nitrocellulose membrane, the membrane was transferred for 1 hour at 100 V (4 °C) followed by blocking in 3% BSA solution in TBS for 1 hour and then overnight incubation (4 °C) with the primary pab240 antibody (1:1000). After washing for 3×10 min with TBS buffer, the membrane was incubated in a solution containing the secondary antibody (Horseradish peroxidase, Caymen

Chemicals) for 3 hours. Thermo Scientific SuperSignal® West Pico Chemiluminescent Substrate kit was used to visualize the mutant p53 protein using a FUJIFILM Luminescent Image Analyzer (LAS-4000). For caspase-3 assays, NUGC3 cells were seeded at a density of 600,000 cells/well and incubated at 37°C with 5% CO₂ for 24 hours, followed by treatment with 25 µM L^I and L^H for 24 hours. SiRNA transfection was performed using 30 nM of siRNA with RNAiMAX (Life Technology) as previously described.¹¹ In the case of co-treatment, cells were incubated with L^I for 2 hours followed by a total 48-hour incubation with oxaliplatin. Cells were lysed with lysis buffer (50 mM Tris-HCl pH 8, NaCl 150 mM, NP40 1%). Proteins were denatured and deposited directly (40 µg of protein) onto an SDS-PAGE gel. For immunoprecipitation, 20µL of the eluates were deposited onto an SDS-PAGE gel. Western blotting was performed using antibodies raised against p53 (Santa Cruz, DO-1, sc-126) and cleaved caspase 3 (Cell Signaling, #9661). Secondary antibodies (anti-rabbit, anti-mouse: GE Healthcare) were incubated according to the manufacturers protocol. Loading was controlled with actin (Chemicon, C4 clone). Signals have been quantified with Genetools software (Syngene) and normalized to actin.

RNA extraction and RT-qPCR. RNA was isolated from NUGC3 cells with 1mL of TRI Reagent (MRC) and RNA was extracted according to the manufacturer's protocol. RNA samples were precipitated with 500µL isopropanol followed by washes with 70% cold ethanol. RNA quality was assessed and 1 µg was used for reverse transcription (High-Capacity cDNA Reverse Transcription Kit, Applied Biosystems). qPCR was performed with performed using a 1:10 dilution of cDNA according to the manufacturer's instructions (LightCycler 480 SYBR Green I Master, Roche), with 500 nM of each primer. The relative expression was calculated using the $\Delta\Delta C_t$ method. Expression levels were normalized using RPLPO.

NCI-60 Screening. Ligands L^I and L^H were submitted to the Developmental Therapeutics Program at the U.S National Cancer Institute for screening on a panel of 60 human tumour cell lines. Compounds are initially tested at a single high dose (10 µM) and those that satisfy pre-determined thresholds will be tested in a five-dose assay.¹² The methodology used in the NCI-60 screen has been described elsewhere.¹³

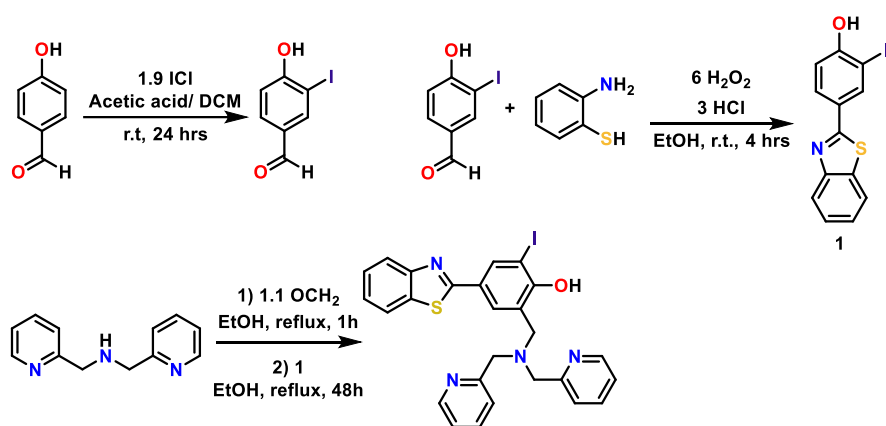
Inhibition of Cell Viability Assay. The *in vitro* cytotoxicity of L^I and L^H against NUGC3 was assayed using the 3-(4,5-dimethylthiazol-2-yl)-2,5-diphenyltetrazolium bromide (MTT) assay.¹⁴ NUGC3 cells were seeded at 10,000 cells per well (100 μ L) in Cellstar 96-well plates (Greiner Bio-One) and incubated at 37 °C with 5% CO₂ for 24 hrs. Following incubation, the cells were exposed to drugs at increasing concentrations ranging from 0.1 to 200 μ M in RPMI medium. Compounds were pre-dissolved in DMSO stocks and serial dilutions were prepared such that the final concentration of DMSO in media was below 1% (v/v). Treated cells were incubated at 37 °C with 5% CO₂ for 48 hrs. Following 48-hr incubation, the MTT test was performed as previously described. Experiments were performed in replicates of eight and repeated at least two times. Inhibition of cell viability was evaluated with reference to determine the absolute IC₅₀ value calculated from dose-response curves using nonlinear variable slope regression (Prism™ software).

Organoid Culture and Immunofluorescence. Small intestinal organoids were obtained from intestinal crypts isolated from a 2-month old female C57BL/6 mouse. They are cultured in a drop of 20 μ L/well Matrigel (Corning) in 48-well plates (Greiner Bio-One) with 250 μ L mouse IntestiCult™ Organoid Growth Medium (StemCell) at 37°C with 5% CO₂. After 3 days, organoids were treated with 2.5 μ M, 5 μ M and 10 μ M of L^I and L^H, and 25 μ M of oxaliplatin. The medium was replaced every 48 hours. For the immunofluorescence experiment, organoids were cultured on 8-well Lab-Tek®II Chamber Slide™ (D. Dutscher). After 24h, 48h and 72h of treatment, organoids were fixed with fixation buffer (Paraformaldehyde 4%, PIPES 60 mM, HEPES 25 mM, EGTA 10 mM, Magnesium acetate 2 mM) for 30 minutes followed by 45-minute quenching (NH₄Cl 50 mM). The organoids were permeabilized for 30 minutes with PBS-Triton 0.5% and blocked with PBS-BSA 5% for 30 minutes. The organoids were incubated for 2 hours at 37°C with Phalloidin-TRITC (Sigma-Aldrich), followed by 10 minutes at 37°C with DAPI (Sigma-Aldrich). Phalloidin is used to reveal actin networks and cellular contours, and DAPI is used to stain DNA. *ca.* 150 organoids were counted and analyzed for each condition. Both observations were done using a fluorescence microscope (Axio Imager M2 Zeiss) coupled to a Hamamatsu's camera Orca Flash 4v3, using the ApoTome.2 (Zeiss) function. Images were analyzed using ImageJ software.

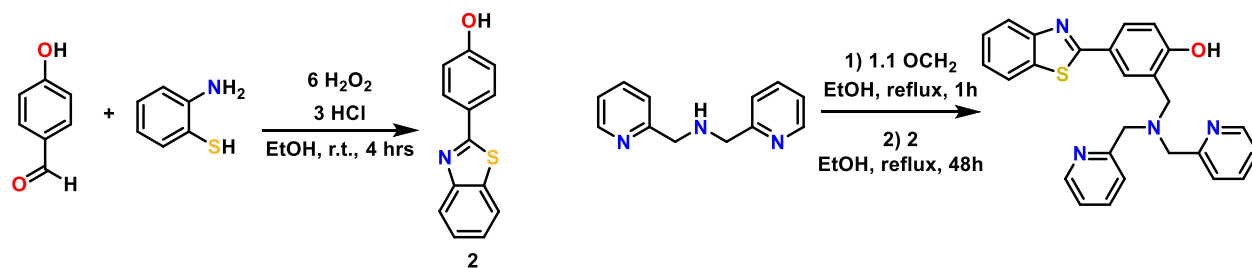
Organoid Survival Assay. For the survival assay experiment, organoids were cultured in 48-well plates (Greiner Bio-one) and treated with L^I and L^H at indicated concentrations. Images of each well were taken every day using a AXIO Zoom.V16 (Zeiss) microscope and analyzed using ImageJ software. Cell Counter plugin was used to distinguish “alive/dead” organoids with or without buddings. Four replicates of each condition were used and 250 organoids per condition were analyzed.

Tolerability of L^I in Normal Mice. The tolerability of L^I has been investigated in C57BL/6 mice treated chronically by intraperitoneal injection twice a week for 5 weeks. Three groups (n=3) have been used to test in parallel three doses of the compound. The dose in each group was increased after 2 weeks of monitoring without any observable secondary effects.

Synthetic Schemes



Scheme S1. Synthesis of L^I.



Scheme S2. Synthesis of L^H.

NMR Characterization

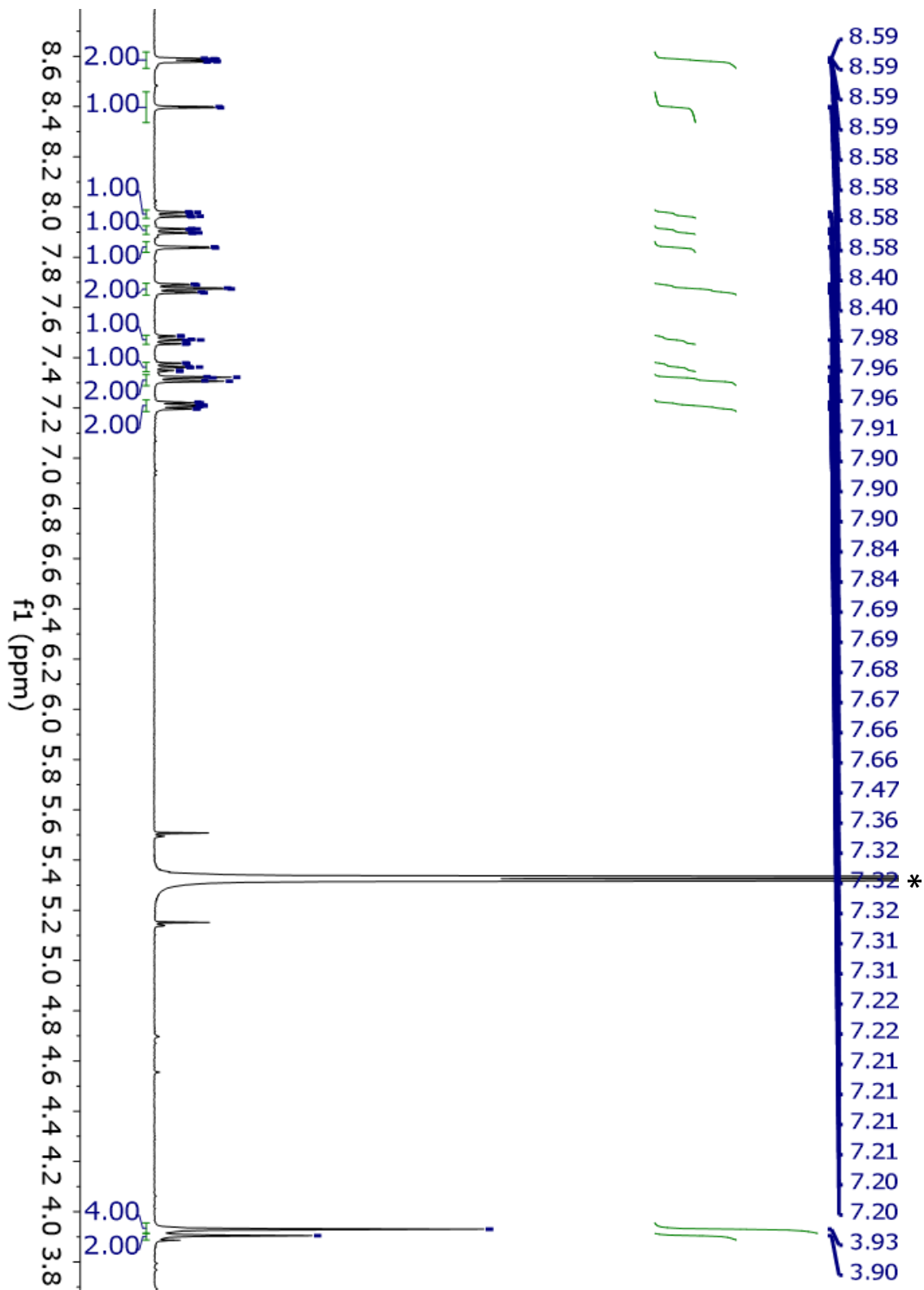


Figure S1. ¹H NMR of L¹ in CD₂Cl₂ (500 MHz). Asterisk denotes residual solvent peak.

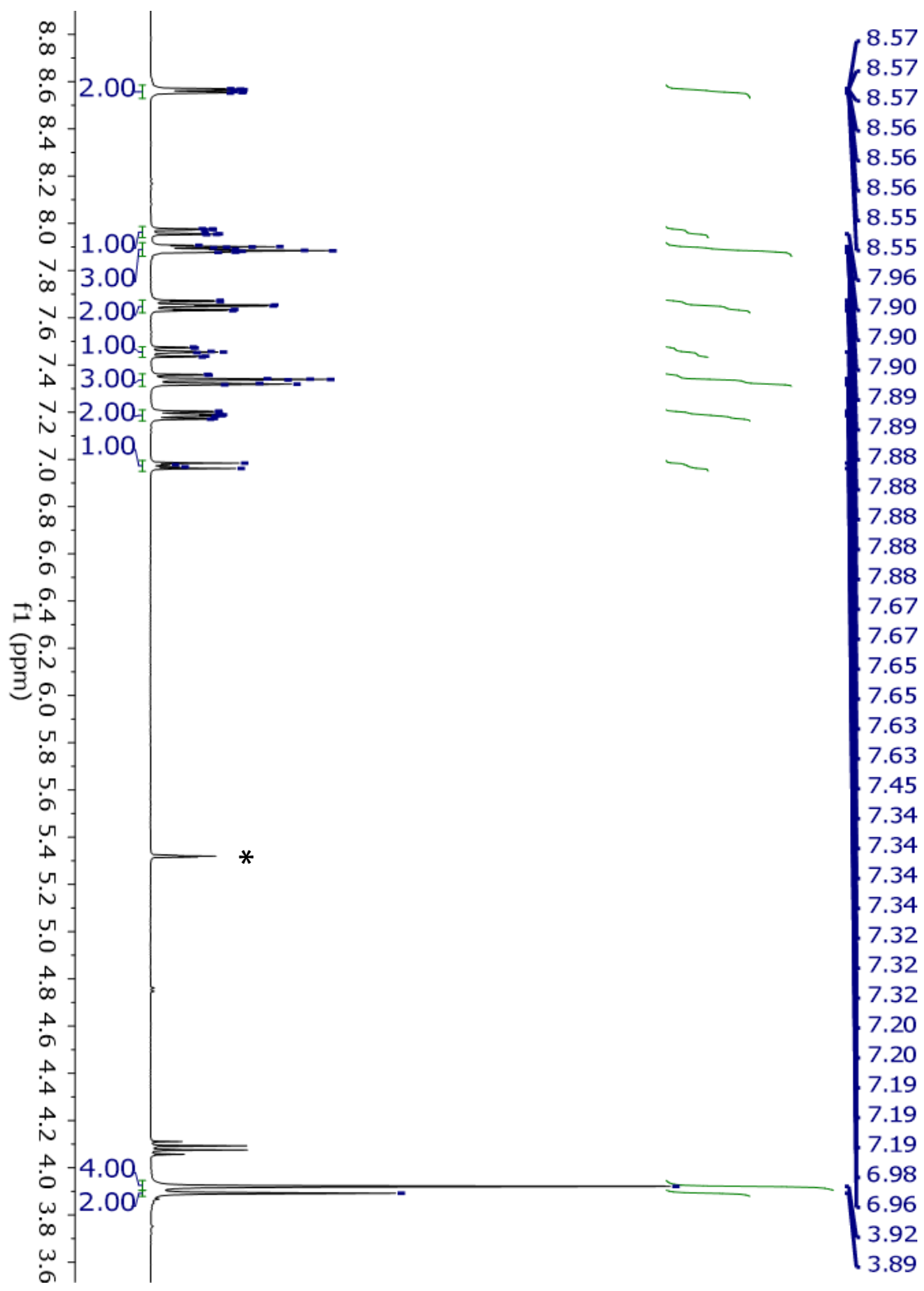


Figure S2. ^1H NMR of L^{H} in CD_2Cl_2 (400 MHz). Asterisk denotes residual solvent peak.

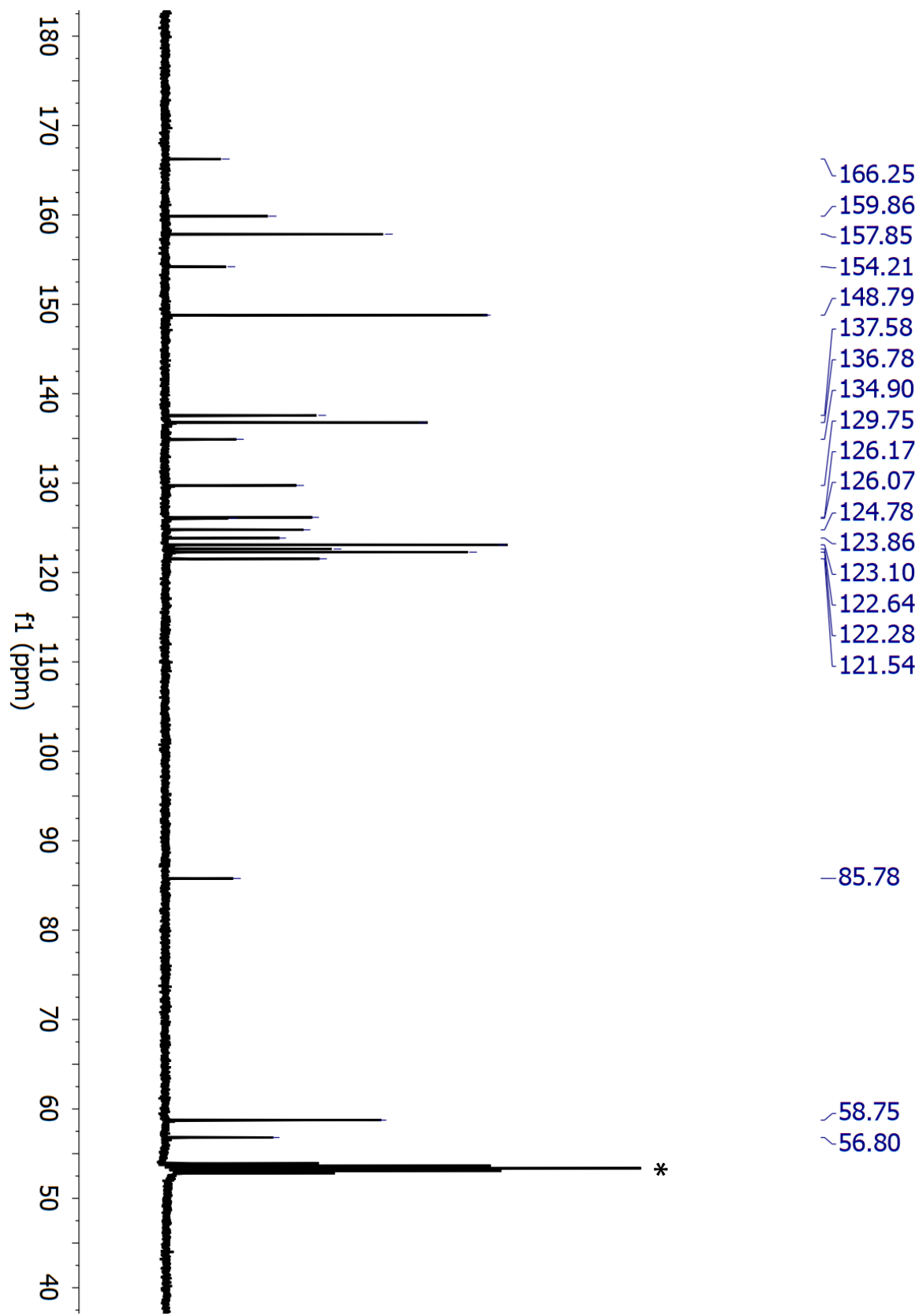


Figure S3. ^{13}C NMR of L^{I} in CD_2Cl_2 (400 MHz). Asterisk denotes residual solvent peak

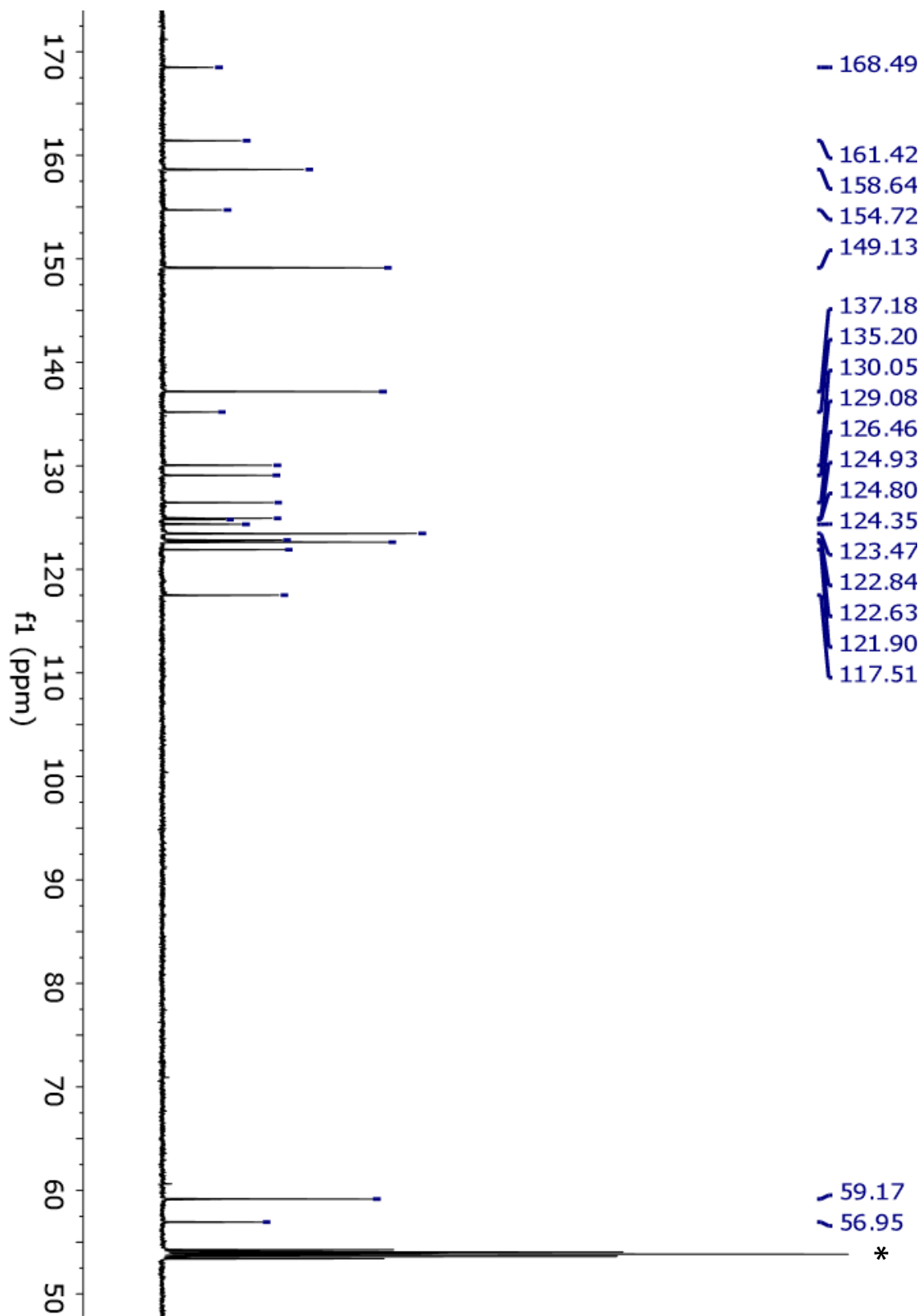


Figure S4. ^{13}C NMR of L^{H} in CD_2Cl_2 (500 MHz). Asterisk denotes residual solvent peak.

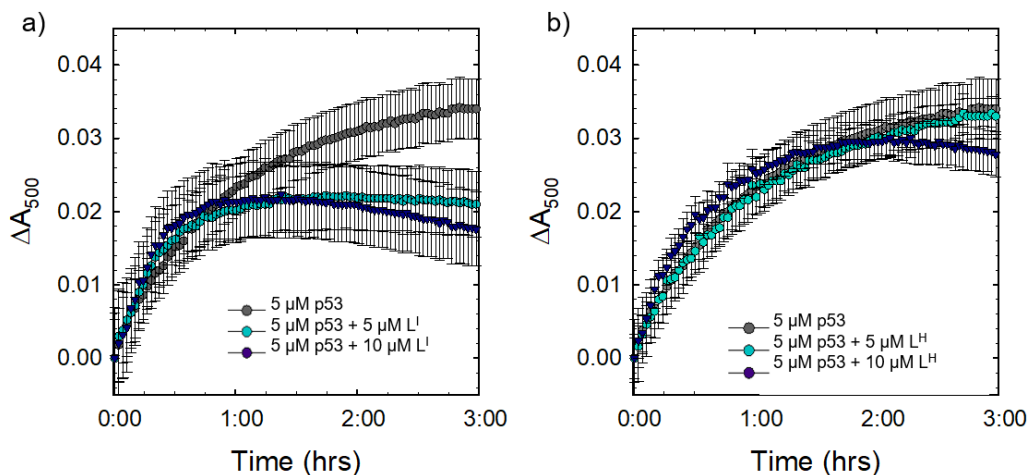


Figure S5. (a) 5 μ M wild-type p53 in 30 mM Tris-HCl, 150 mM NaCl, pH 7.4 was incubated at 37 $^{\circ}$ C. Light scattering at 500 nm was monitored over time from 0 to 3 hours. Absorbance readings were recorded every 3 minutes, with 30 seconds of agitation before each reading. Addition of 5 and 10 μ M of L^I shows inhibition of aggregation. (b) Addition of 5 and 10 μ M of L^H results in no significant changes in p53 aggregation.

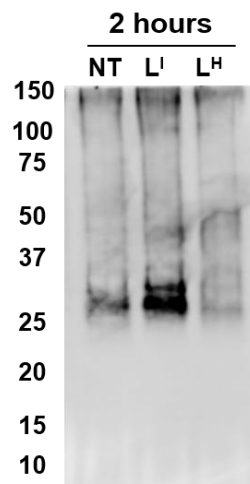


Figure S6. L^I modulates the molecular weight distribution of mutant p53-y220c. Gel electrophoresis and Western blot of 8 μ M p53-y220c in 30 mM Tris, 150 mM NaCl, pH 7.4 (NT – lane 1) and two equivalents of L^I (lane 2) and L^H (lane 3) after a 2-hour incubation with constant agitation at 37 $^{\circ}$ C. Western blot was revealed using the primary antibody pab240, which recognizes mutant p53.

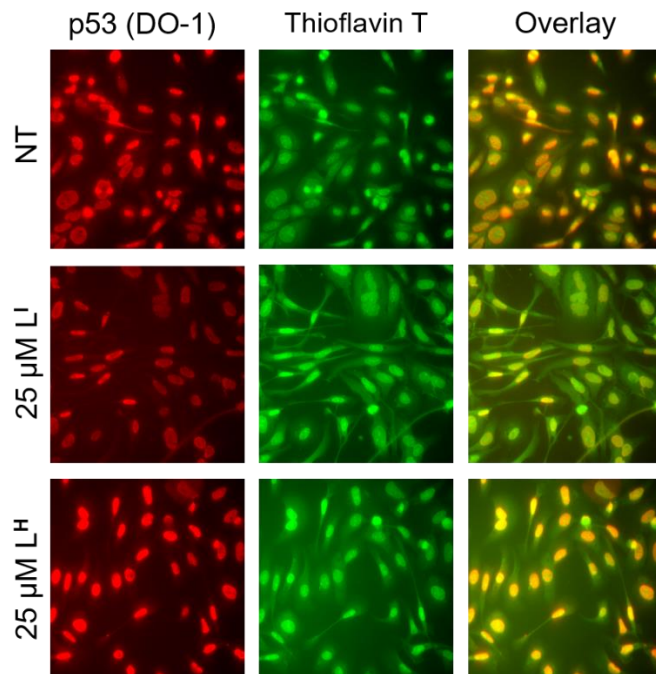


Figure S7. Overlay between Thioflavin T staining and p53 is reduced in mutant p53 cell line NUGC3 after treatment with L^I . NUGC3 cells were treated with 25 μM L^I/L^H or 0.1% DMSO (NT) for 24 hours followed by labelling with anti-p53 primary antibody DO-1 (1:1000) and ThT (1 mM). Images were obtained using a fluorescence microscope. Columns from left to right include: DO-1 (anti-p53), ThT, and co-immunofluorescence of DO-1 and ThT.

pKa Determination

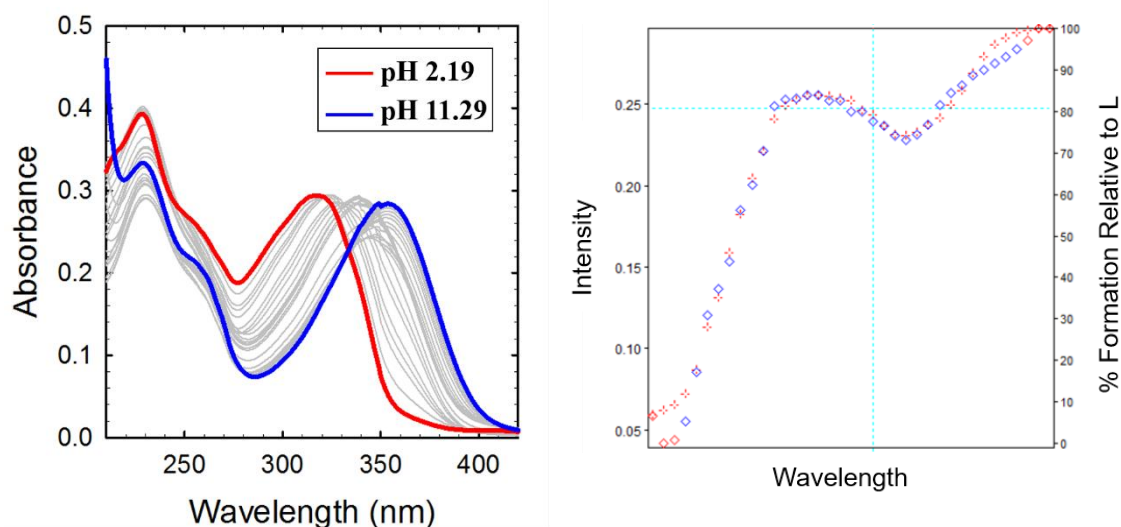


Figure S8. (left) Variable pH UV-vis titration of 12.5 μM L^I ranging from pH 2.19-11.29 in 0.1 M NaCl. (right) Absorbance trace at 353 nm as a function of pH. Observed absorbance values are shown in red, calculated absorbance values are in blue.

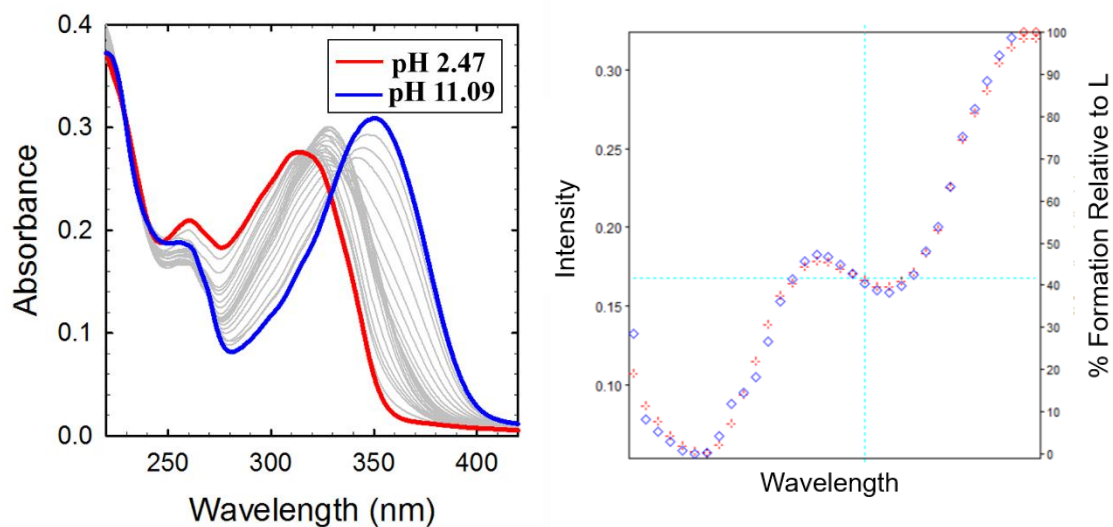


Figure S9. (left) Variable pH UV-vis titration of $12.5 \mu\text{M } L^H$ ranging from pH 2.47-11.09 in 0.1 M NaCl. (right) Absorbance trace at 350 nm as a function of pH. Observed absorbance values are shown in red, calculated absorbance values are in blue.

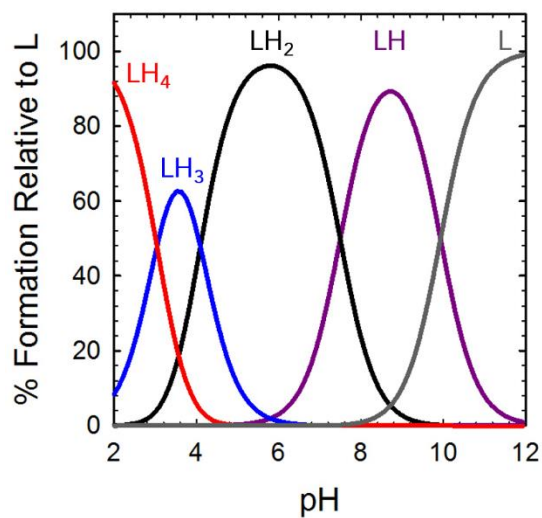


Figure S10. Simulated species distribution plot for L^I using HypSpec and HySS2009.

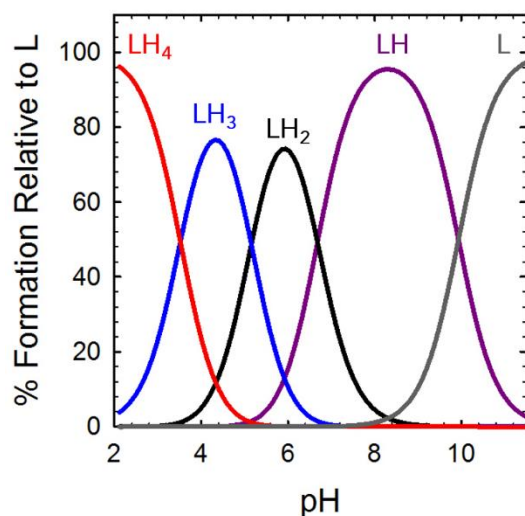


Figure S11. Simulated species distribution plot for L^H using HypSpec and HySS2009.

Zn K_d Determination

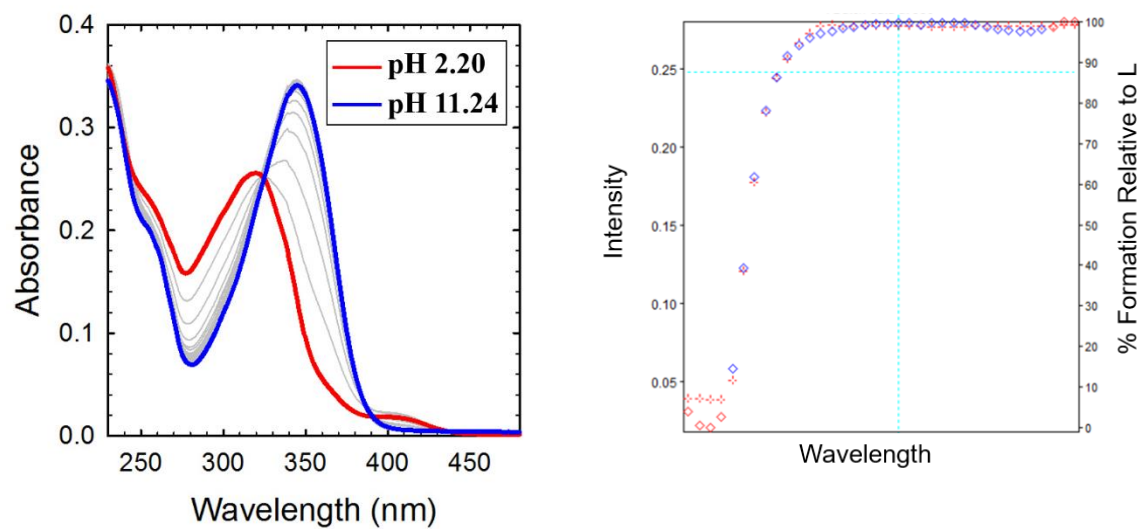


Figure S12. (left) Variable pH titration curve of $12.5 \mu\text{M Zn}^{2+} + 12.5 \mu\text{M L}^I$ ranging from pH 2.20-11.24 in 0.1 M NaCl. (right) Absorbance trace at 359 nm as a function of pH. Observed absorbance values are shown in red, calculated absorbance values are in blue.

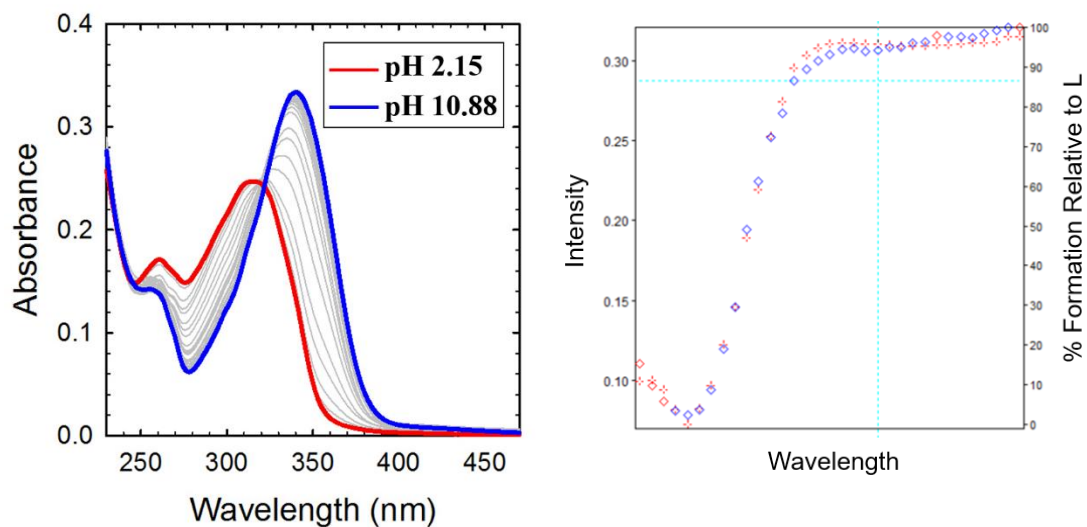


Figure S13. (left) Variable pH titration curve of $12.5 \mu\text{M Zn}^{2+} + 12.5 \mu\text{M L}^{\text{H}}$ ranging from pH 2.15-10.88 in 0.1 M NaCl. (right) Absorbance trace at 346 nm as a function of pH. Observed absorbance values are shown in red, calculated absorbance values are in blue.

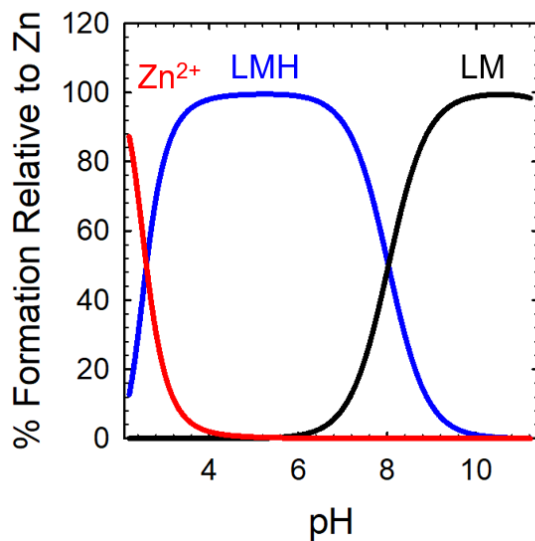


Figure S14. Simulated species distribution plot of $\text{Zn}^{2+} + \text{L}^{\text{I}}$ using HySS2009.

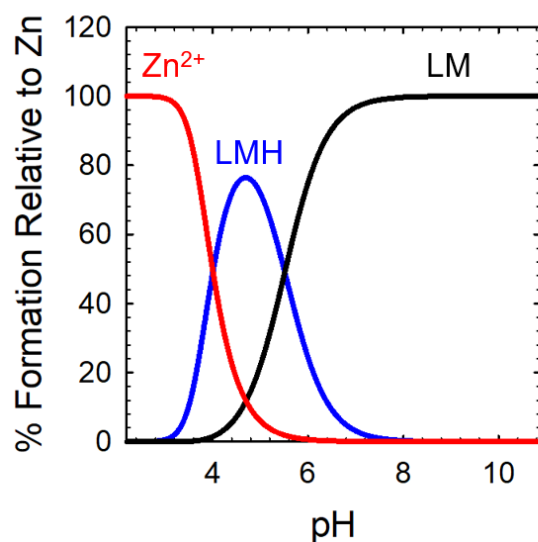


Figure S15. Simulated species distribution plot of $\text{Zn}^{2+} + \text{L}^{\text{H}}$ using HySS2009.

Table S1. pKa values as determined by variable pH UV-vis titrations (errors are for the last digit).

Reaction	L^{I}	L^{H}
$[\text{HL}] = [\text{L}]^{-} + \text{H}^{+}$ ($\text{p}K_{\text{a1}}$)	2.98(2)	1.13(2)
$[\text{H}_2\text{L}]^{+} = [\text{HL}] + \text{H}^{+}$ ($\text{p}K_{\text{a2}}$)	4.10(1)	4.78(2)
$[\text{H}_3\text{L}]^{2+} = [\text{H}_2\text{L}]^{+} + \text{H}^{+}$ ($\text{p}K_{\text{a3}}$)	7.488(9)	7.05(2)
$[\text{H}_4\text{L}]^{3+} = [\text{H}_3\text{L}]^{2+} + \text{H}^{+}$ ($\text{p}K_{\text{a4}}$)	9.928(5)	9.937(2)

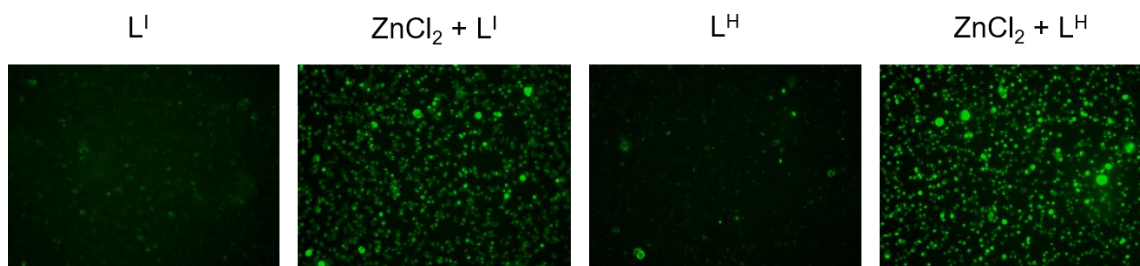
Table S2. Stability constants ($\log K$) of the Zn complexes of L^{I} and L^{H} and calculated pM values^[a] (errors are for the last digit).

	pZn ^[a] (pH 7.4)	Log K	
		ZnL	ZnLH
L^{I}	8.4	14.1	8.0
L^{H}	8.2	13.9	5.5

^[a]pZn was calculated using $\text{pZn} = (-\log[\text{Zn}^{2+}]_{\text{free}})$, where Zn^{2+} is determined from the Hyss model.¹⁵ $[\text{L}^{\text{I}}$ and $\text{L}^{\text{H}}] = [\text{Zn}^{2+}] = 12.5 \mu\text{M}$, 25 °C, I = 150 mM NaCl.

Table S3. Selected crystallographic information for ZnL^ICl and ZnL^HCl.

Crystallographic Information	ZnL ^I Cl	ZnL ^H Cl
Formula	C ₂₆ H ₂₀ ClIN ₄ OSZn	C ₂₆ H ₂₁ ClIN ₄ OSZn
Formula Weight	664.27	538.38
Space Group	P2 ₁ /c	P -1
<i>a</i> (Å)	15.51(2)	13.30(6)
<i>b</i> (Å)	13.17(2)	14.24(7)
<i>c</i> (Å)	14.73(2)	15.81(8)
α (deg)	90	101.7(2)
β (deg)	116.8(10)	99.1(3)
γ (deg)	90	99.5(2)
V [Å ³]	2685.15	2832.98
Z	4	21
T (K)	293	150
ρ_{calcd} (g cm ⁻³)	1.643	1.454
λ (Å)	1.54178	1.54178
μ (cm ⁻¹)	12.148	3.163
R indices ^a with I > 2.0 σ (I) (data)	0.0245	0.0784
wR ₂	0.0645	0.1945
R ₁	0.0263	0.0819
Goodness-of-fit on F ²	1.050	1.099
^a Goodness-of-fit on <i>F</i>		

**Figure S16.** Both ZnCl₂ and L^I/L^H are required for intracellular uptake. Imaging of intracellular Zn²⁺ levels in complete serum-free media. NUGC3 cells were incubated with 1 μ M FZ3-AM for 20 minutes at 37°C, followed by incubation with 50 μ M L^I and L^H for 2 hours. Cells were imaged using a fluorescence microscope and fluorescence-quantified using ImageJ.

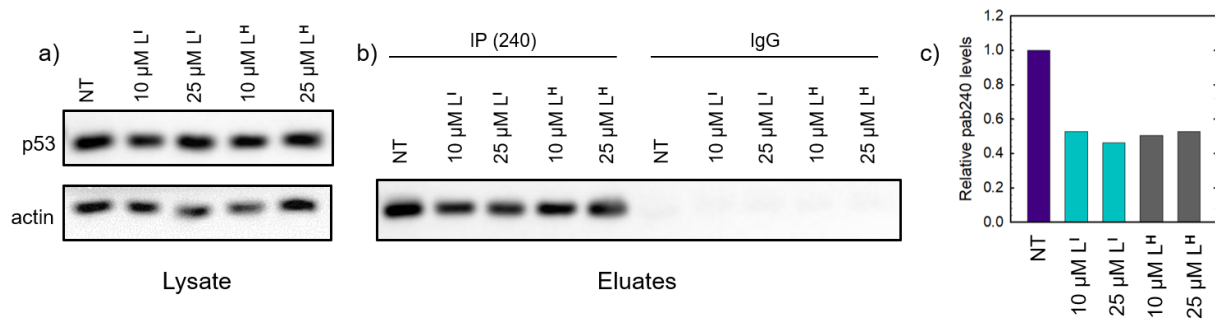


Figure S17. Mutant p53 levels are reduced upon treatment with L^I and L^H. NUGC3 cells were treated for 13 hours with L^I and L^H at the indicated concentrations. Cells were then lysed and proteins were immunoprecipitated using the p53 antibody pAb240 that immunoprecipitates only mutated p53. Precipitated proteins were separated on a 10% SDS page gel and incubated with the p53 antibody (DO-1), which recognizes both mutated and wild-type p53. An unrelated antibody was used as a negative control for immunoprecipitation (IgG). Actin protein levels present in the lysate are shown as a control for the amount of protein used in the immunoprecipitation. (a) representative Western blot image of lysate conditions added to the pAb240 antibody prior to immunoprecipitation (b) representative Western blot image of eluate samples removed post immunoprecipitation (c) Quantification of relative pAb240 antibody levels from eluates in part (b).

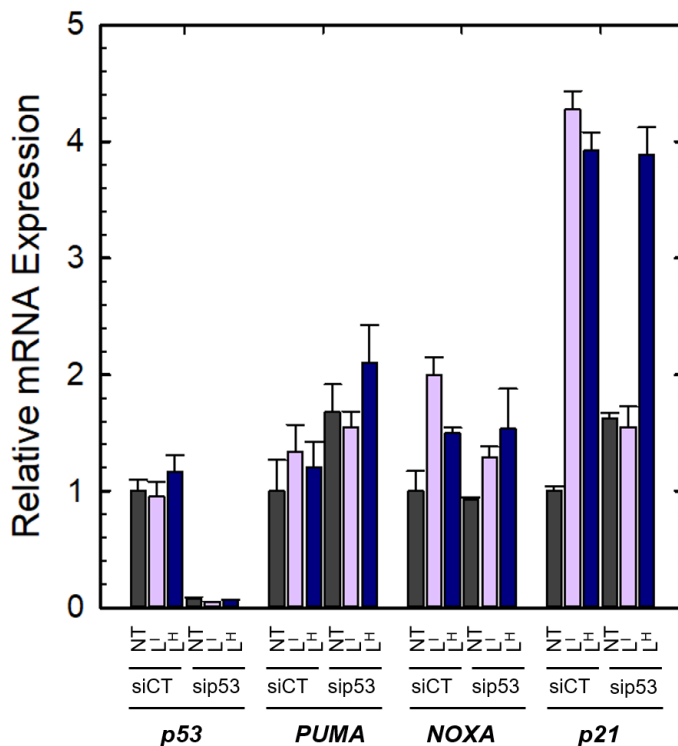


Figure S18. NUGC3 cells were transfected with control siRNA (siCT) or siRNA directed against p53 (sip53) and then treated for 6 hours with 25 μM of L^I and L^H. Total RNAs were extracted and RT-qPCR performed to measure the expression of TP53 (p53), P21, PUMA and NOXA. Bars represent means of triplicates with error bars.

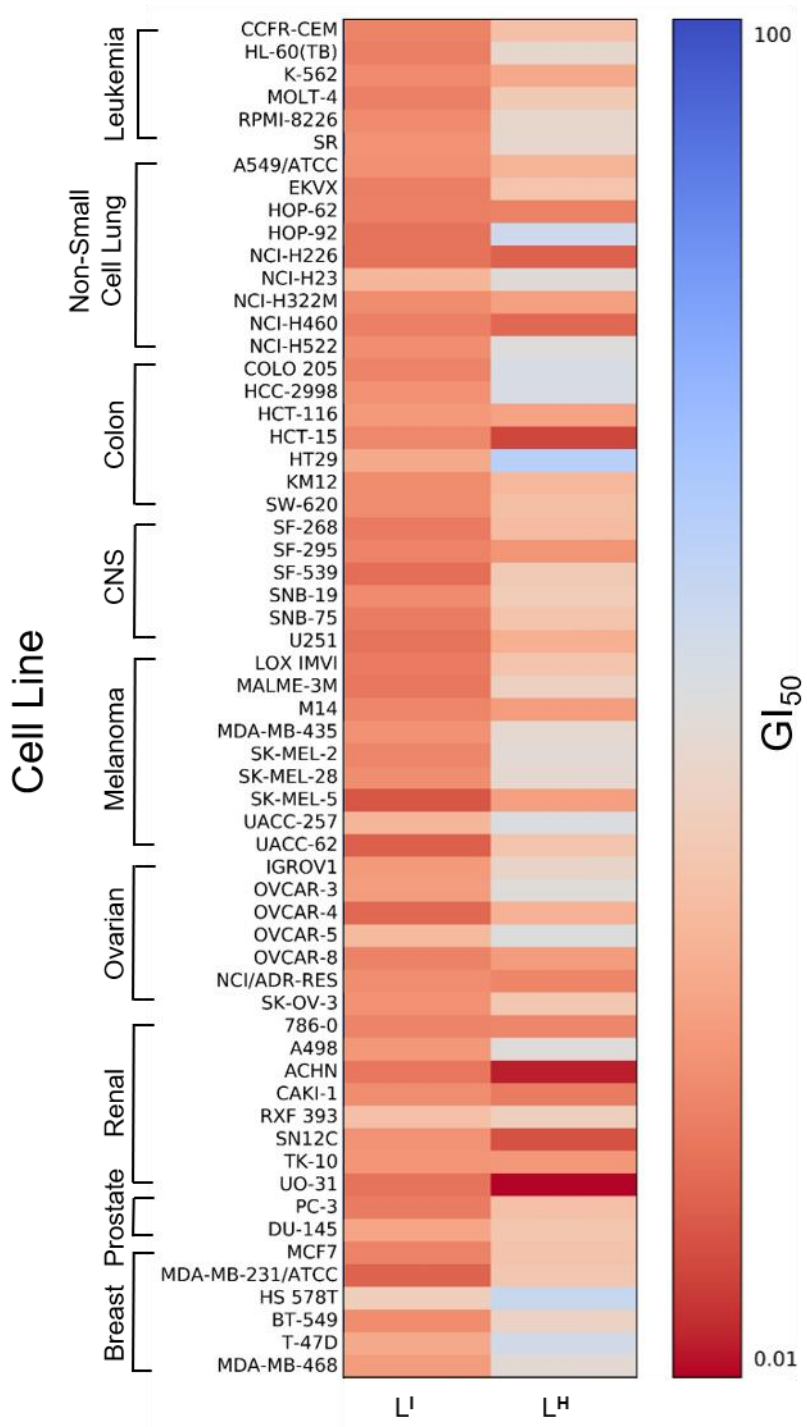


Figure S19. Heat map showing the *in vitro* cytostatic activity ($\log_{10} GI_{50}$) of L^I and L^H in the NCI-60 screen. Blue indicates low cytotoxicity (100 μ M) and red indicates high cytotoxicity (0.01 μ M).

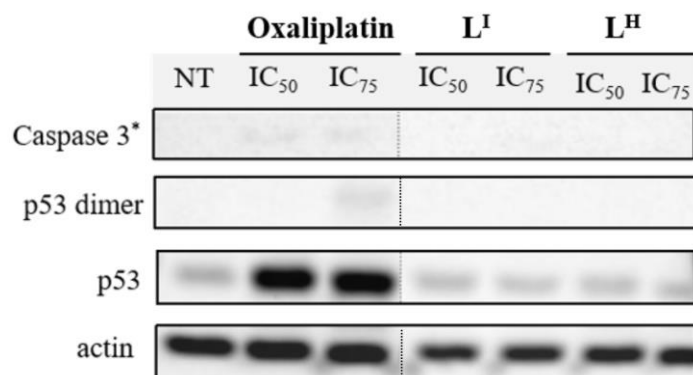
Table S4. Mean GI₅₀ and LC₅₀ values from the NCI-60 screen.

Ligand	NSC Number ^[a]	GI ₅₀ (μM) ^[b]	LC ₅₀ (μM) ^[b]
L ^I	788648	0.44	93.8
L ^H	788649	1.58	79.2
Cisplatin ¹⁶	119875	1.5	44.0
Oxaliplatin ¹⁶	226046	2.8	> 90

^[a] NSC number is the compounds internal ID number at the National Cancer Institute. ^[b] GI₅₀ values correspond to the dose that inhibits 50% of cell growth compared to non-treated controls, while LC₅₀ indicates the concentration required to kill 50% of treated cells.¹³

Table S5. IC₅₀ values for stomach cancer cell line NUGC3 upon indicated treatment for 48 hours.

Ligand	NUGC3 (p53 ^{Y220C})
L ^I	4.5 ± 0.9
L ^H	24.6 ± 3.4
Cisplatin	20.0 ± 1.7
Oxaliplatin	50.0 ± 2.7

**Figure S20.** Neither L^I or L^H treatment results in cleavage of caspase-3 in AGS (wtp53) cells. AGS cells were treated with IC₅₀ and IC₇₅ concentrations of indicated compound for 24 hours. Proteins were extracted, and 40 μg were separated on SDS PAGE. Cleaved caspase-3 (Caspase 3*), p53, and actin were detected by Western blot.

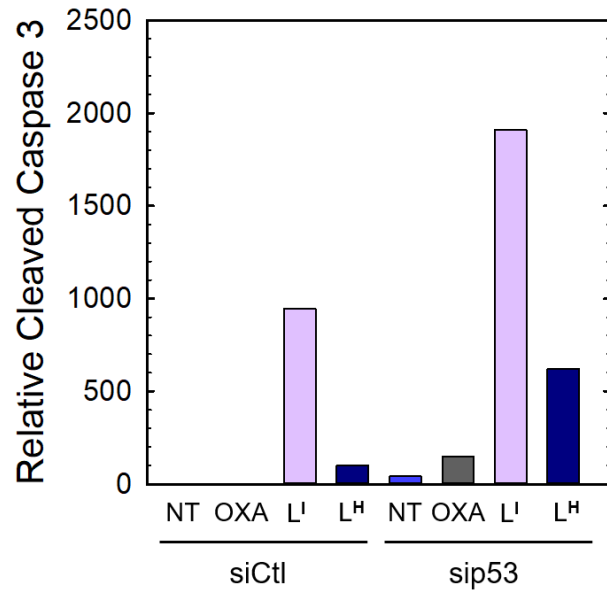


Figure S21. Quantification of relative caspase 3 levels obtained by Western blot analysis upon treatment with oxaliplatin, L^I, and L^H. Western blot image quantified using SynGene tools.

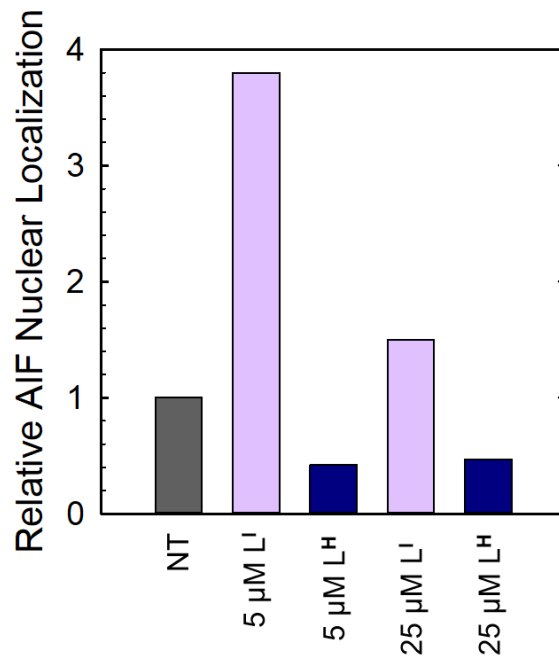


Figure S22. Quantification of relative AIF nuclear localization obtained by immunofluorescence.

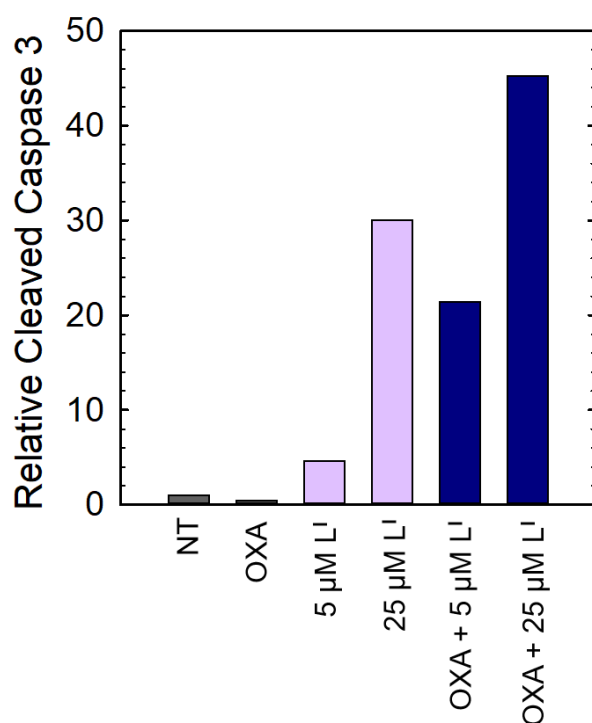


Figure S23 Quantification of relative caspase 3 levels obtained by Western blot analysis upon cotreatment with L¹ and oxalipatin. Western blot image quantified using SynGene tools.

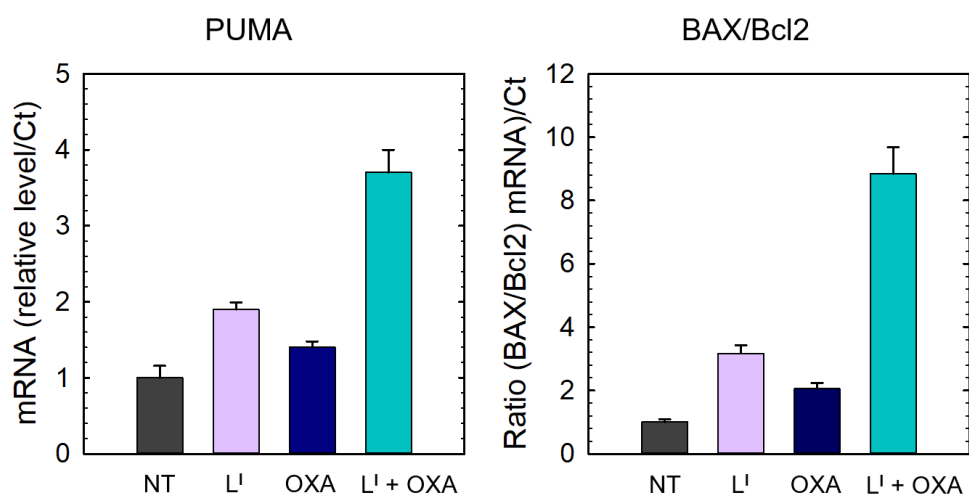


Figure S24. Cotreatment with L¹ and oxalipatin results in increased activation of apoptosis over treatment with L¹ or oxalipatin alone. NUGC3 cells were treated with 10 μM of indicated compound for 48 hours. In the case of cotreatment, cells were incubated with L¹ for 2 hours followed by a total 24-hour incubation. RNAs were extracted and RT-qPCR for *PUMA*, *BAX*, and *BCL2* mRNAs quantification were performed. Graph represent means with error bars of mRNA expression relative to Ct. *BAX* and *BCL2* are represented as a ratio of their relative expression that is representative of cell death activation.

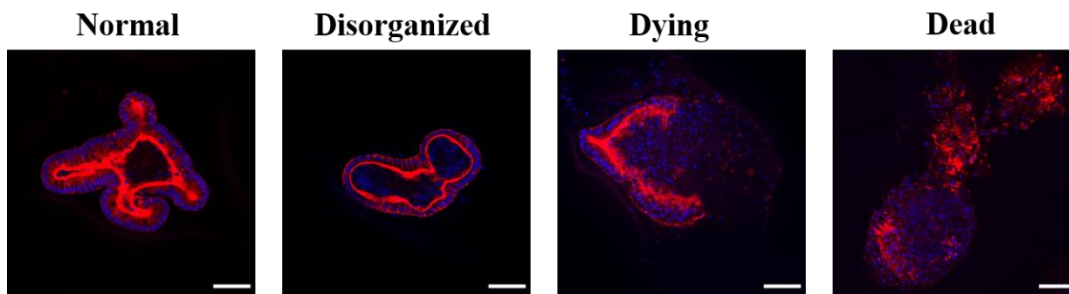


Figure S25. Intestinal organoids were incubated and monitored for 72 hours. F-actin (red) and nuclei (blue) were stained using Phalloidin and DAPI respectively at recommended concentrations and imaged using a Zeiss ApoTome microscope. Organoids were then classified as normal, disorganized, dying, or dead based on cell morphology. Representative images for each classification condition are shown above. The scale bar represents 50 μM .

Table S6. Number of organoids counted in each classification system per indicated treatment condition.

Treatment	Normal	Disorganized	Dying	Dead	Total
NT	84	35	20	6	145
25 μM OXA	0	87	42	36	165
2.5 μM L ^I	64	45	11	10	130
5 μM L ^I	77	70	27	16	190
10 μM L ^I	41	76	33	11	161
2.5 μM L ^H	41	63	30	27	161
5 μM L ^H	0	27	45	64	136
10 μM L ^H	0	0	0	166	166

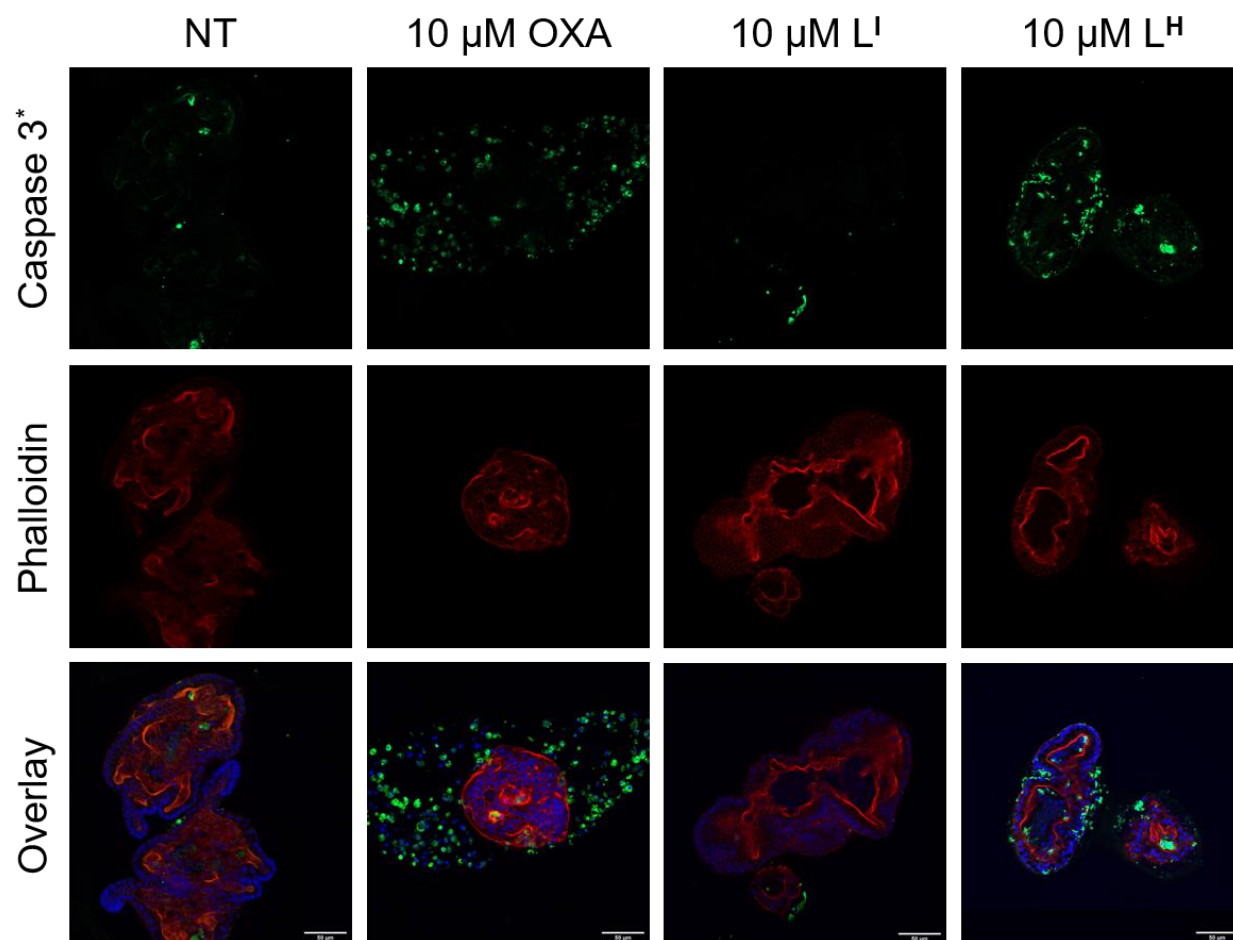


Figure S26. Treatment of non-cancerous intestinal organoids results in increased cleavage of caspase 3 with L^H compared to L^I, indicating that L^H induces apoptosis in non-cancerous organoids. Intestinal organoids were treated with indicated compound for 24 hours. F-actin (red) and nuclei (blue) were stained using Phalloidin and DAPI respectively. Apoptotic cells are stained using cleaved caspase 3 (green). Antibodies were used at recommended concentrations and imaged using a Zeiss ApoTome microscope. The scale bar represents 50 μ M.

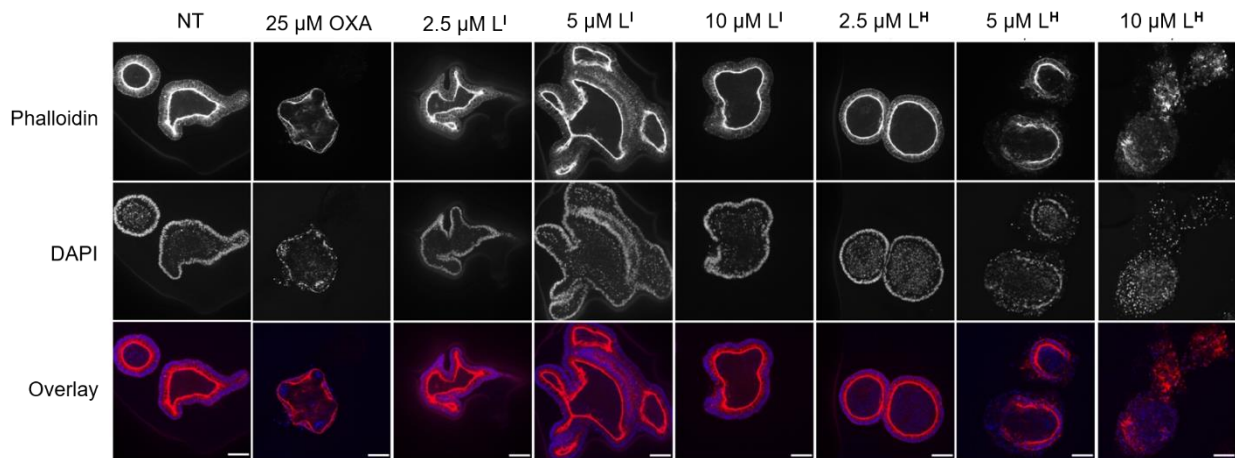
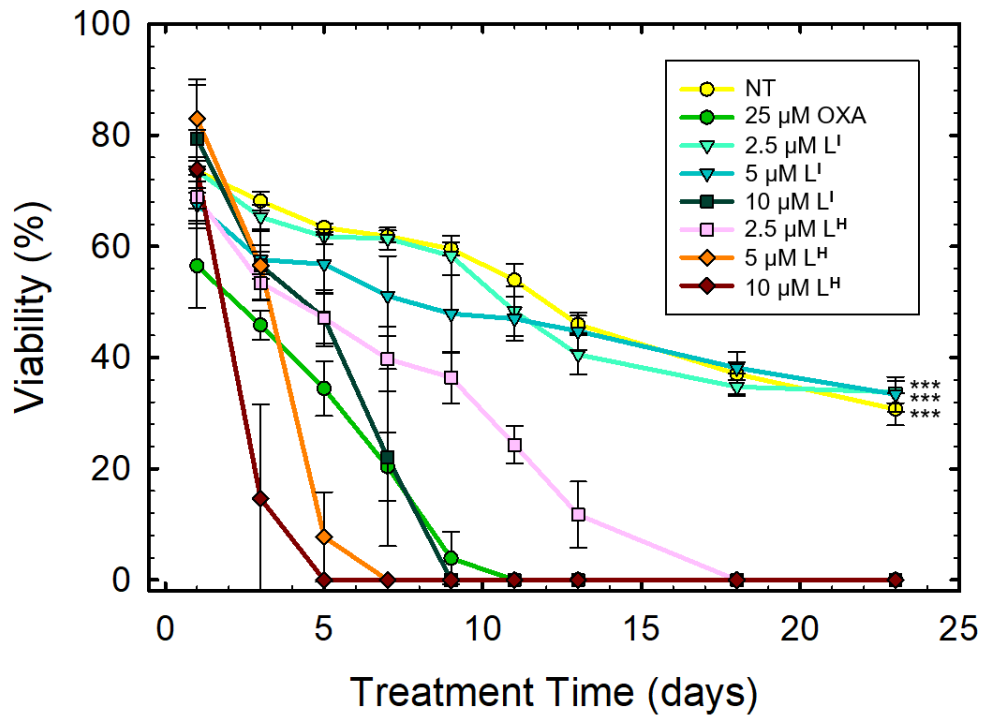


Figure S27. Treatment of non-cancerous intestinal organoids results in increased survival upon treatment with L^I compared to L^H. Intestinal organoids were treated with indicated compound and monitored for 23 days. F-actin (red) and nuclei (blue) were stained using Phalloidin and DAPI respectively at recommended concentrations and imaged using a Zeiss ApoTome microscope. Characterization and quantification of organoids as either normal, disorganized, dying or dead upon indicated treatment based on images obtained from 4 replicates. Graph shows survival curves for each condition. *** indicates $p < 0.001$ established by anova followed by a Dunnett post-test. The scale bar represents 50 μM .

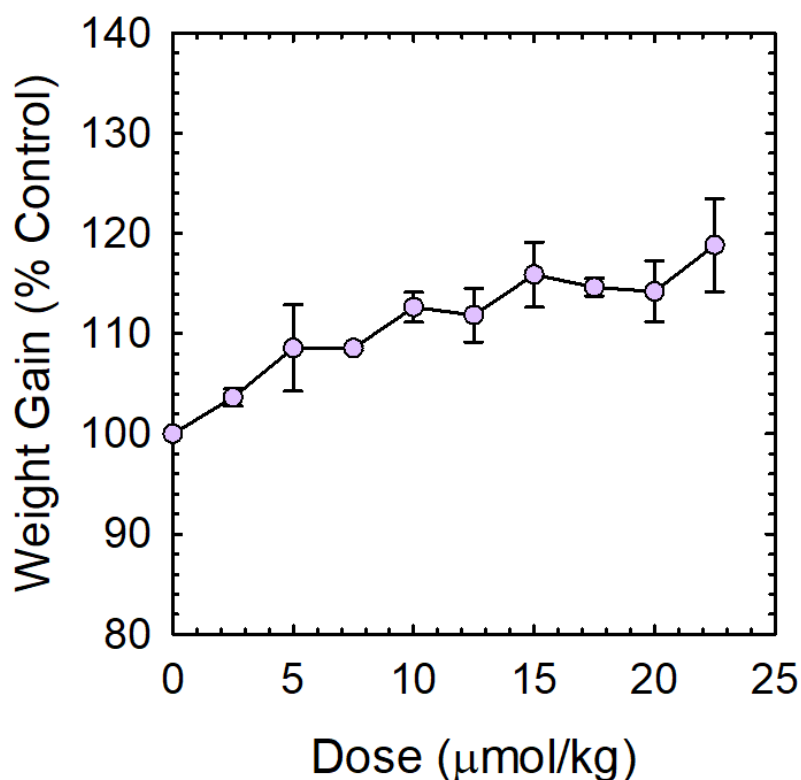


Figure S28. L^I is well tolerated in normal mice as no weight loss is observed with increasing concentrations. C57BL/6 mice were injected intraperitoneally with increasing doses (µmol/kg) of L^I and monitored twice a week for five weeks. Mean weight of mice (three groups with n=3) are shown as averages ± SD.

References

- 1.(a) Kieboom, A. P. G., *Recueil des Travaux Chimiques des Pays-Bas* **1988**, *107*, 685; (b) Perrin, D. D.; Armarego, W. L. F., *Purification of Laboratory Chemicals*. 1st ed. ed.; Pergamo Press: New York, 1988.
- 2.Sheldrick, G. M., *SHELXT v2014*; , Bruker AXS Inc: Madison, WI.
- 3.Hübschle, C. B.; Sheldrick, G. M.; Dittrich, B., ShelXle: a Qt graphical user interface for SHELXL. *J. Appl. Crystallogr.* **2011**, *44* (Pt 6), 1281-1284.
- 4.Gans, P.; Sabatini, A.; Vacca, A., Determination of Equilibrium Constants from Spectrophotometric Data Obtained from Solutions of Known pH: The Program pHab. *Ann. Chim.* **1999**, *89*, 45-49.
- 5.Baes, C. F. J.; Mesmer, R. E., *The Hydrolysis of Cations*. R. E. Krieger Publishing Co: Malabar, FL, 1986.
- 6.Gee, K. R.; Zhou, Z. L.; Ton-That, D.; Sensi, S. L.; Weiss, J. H., Measuring zinc in living cells.: A new generation of sensitive and selective fluorescent probes. *Cell Calcium* **2002**, *31* (5), 245-251.
- 7.Ayed, A.; Mulder, F. A. A.; Yi, G.-S.; Lu, Y.; Kay, L. E.; Arrowsmith, C. H., Latent and active p53 are identical in conformation. *Nat. Struct. Mol. Biol.* **2001**, *8* (9), 756-760.
- 8.Nikolova, P. V.; Henckel, J.; Lane, D. P.; Fersht, A. R., Semirational design of active tumor suppressor p53 DNA binding domain with enhanced stability. *Proc. Natl. Acad. Sci. U. S. A.* **1998**, *95* (25), 14675-14680.
- 9.Bullock, A. N.; Henckel, J.; DeDecker, B. S.; Johnson, C. M.; Nikolova, P. V.; Proctor, M. R.; Lane, D. P.; Fersht, A. R., Thermodynamic stability of wild-type and mutant p53 core domain. *Proc. Natl. Acad. Sci. U. S. A.* **1997**, *94* (26), 14338-14342.

10. Gill, S. C.; von Hippel, P. H., Calculation of protein extinction coefficients from amino acid sequence data. *Anal. Biochem.* **1989**, *182* (2), 319-326.
11. von Grabowiecki, Y.; Abreu, P.; Blanchard, O.; Palamiuc, L.; Benosman, S.; Mériaux, S.; Devignot, V.; Gross, I.; Mellitzer, G.; Gonzalez de Aguilar, J. L.; Gaiddon, C., Transcriptional activator TAp63 is upregulated in muscular atrophy during ALS and induces the pro-atrophic ubiquitin ligase Trim63. *eLife* **2016**, *5*, e10528-e10548.
12. Paull, K. D.; Shoemaker, R. H.; Hodes, L.; Monks, A.; Scudiero, D. A.; Rubinstein, L.; Plowman, J.; Boyd, M. R., Display and Analysis of Patterns of Differential Activity of Drugs Against Human Tumor Cell Lines: Development of Mean Graph and COMPARE Algorithm. *J. Natl. Cancer Inst.* **1989**, *81* (14), 1088-1092.
13. Shoemaker, R. H., The NCI60 human tumour cell line anticancer drug screen. *Nat. Rev. Cancer* **2006**, *6* (10), 813-823.
14. Mosmann, T., Rapid colorimetric assay for cellular growth and survival: Application to proliferation and cytotoxicity assays. *J. Immunol. Methods* **1983**, *65* (1), 55-63.
15. Alderighi, L.; Gans, P.; Ienco, A.; Peters, D.; Sabatini, A.; Vacca, A., Hyperquad simulation and speciation (HySS): a utility program for the investigation of equilibria involving soluble and partially soluble species. *Coord. Chem. Rev.* **1999**, *184* (1), 311-318.
16. Holbeck, S. L.; Collins, J. M.; Doroshow, J. H., Analysis of Food and Drug Administration-approved anticancer agents in the NCI60 panel of human tumor cell lines. *Mol. Cancer Ther.* **2010**, *9* (5), 1451-1460.